

Detection and evaluation of single bubble collisions using focused shadowgraphy

Erkennung und Auswertung von Blasenkollisionen mithilfe der fokussierten Schattenmethode

E. Frense, T. Werner, J.-A. Nöpel, F. Rüdiger

Institute of Fluid Mechanics, Technische Universität Dresden, 01069 Dresden

Bubble interaction, high-speed imaging, image processing

Blaseninteraktion, Hochgeschwindigkeitsaufnahmen, Bildverarbeitung

Abstract

Recent research in multiphase flow addresses the experimental investigation of bubble interaction like coalescence and breakup in pipe systems with low void fractions found in typical industrial applications. As the main experimental technique high-speed focused shadowgraphy is used, combined with image processing. The modelling of bubble interaction requires the reliable detection of events such as the collision between two bubbles. Therefore, an image processing algorithm was developed which enables the detection of potential collisions. By performing dilation of labelled objects, overlapping regions indicate approaching bubbles. Given a sufficiently well recorded event it is possible to evaluate the bubble dynamics. Unfortunately, this routine does not allow the distinction of at the one hand contactless overlapping of bubbles with an increased distance in depth direction and at the other hand real collisions of nearby bubbles. To get the information on the coordinate in depth direction, an optical setup with a small depth of field is applied. This leads to a blur of bubble edges with increasing distance to the focal plane. A prior generated calibration function allows evaluating the coordinate in depth direction for blurred bubbles. Proving of the accuracy of the presented method is carried out by imaging from an additional 90-degree view. Hence, it allows to determine a detected potential bubble collision as being a real collision.

Zusammenfassung

Aktuelle Forschungsarbeiten auf dem Gebiet der Mehrphasenströmung befassen sich mit der experimentellen Untersuchung von Blaseninteraktionen wie Koaleszenz und Aufbrechen in Rohrsystemen mit geringer Blasenbeladung, wie sie typischerweise in industriellen Anwendungen vorkommen. Als wichtigste experimentelle Methode werden fokussierte Hochgeschwindigkeits-Schattenaufnahmen in Verbindung mit Bildverarbeitung eingesetzt. Die Modellierung der Blaseninteraktion erfordert die zuverlässige Erkennung von Ereignissen wie die Kollision zwischen zwei Blasen. Daher wurde ein Bildverarbeitungsalgorithmus entwickelt, der die Erkennung potenzieller Kollisionen ermöglicht. Durch künstliches Aufdicken aller detektierten Objekte entstehen bei geringem Abstand zwischen zwei Objekten Überlappungsbereiche, die erkannt werden können. Bei einem zeitlich und örtlich hinreichend gut aufgezeichneten Ereignis ist es möglich, die Blasendynamik auszuwerten. Bisher ist bei diesem Ansatz keine

Unterscheidung zwischen einem berührungslosen Überlappen von Blasen mit erhöhtem Abstand in Tiefenrichtung und Kollisionen nahe beieinander liegender Blasen möglich. Um die Information über die Koordinate in Tiefenrichtung zu erhalten, wird ein optischer Aufbau mit geringer Tiefenschärfe verwendet. Dies führt zu einer Unschärfe der Blasenkonturen mit zunehmendem Abstand zur Fokusebene. Eine zuvor generierte Kalibrierungsfunktion ermöglicht die Bestimmung der Koordinate in Tiefenrichtung. Der Nachweis der Genauigkeit der vorgestellten Methode erfolgt durch Referenzaufnahmen aus einer zusätzlichen, um 90° gedrehten Betrachtungsrichtung. Darüber hinaus wird ermöglicht, eine detektierte potenzielle Blasenollision als Kollision zu klassifizieren.

Introduction

To achieve a better understanding of bubble interaction in pipe systems, it is necessary to investigate effects like coalescence or breakup depending on the present flow configuration. For that purpose, a test facility was designed and constructed being able to study the multiphase flow in a T-junction using high-speed imaging. The present flow is three dimensional which can lead to deformation and transport of bubbles in all three dimensions. Therefore, 2D measurement techniques like the focused shadowgraphy give too little information compared to stereoscopic imaging but are often the only option in terms of cost efficiency or limited optical accessibility.

Many approaches are investigated in the literature to extract additional information from 2D imaging based on specific effects of the optical system via calibration. One example is the change of shape of μ PIV tracer particles depending on the position on the optical axis when using a cylindrical lens in the setup (Cierpka et al. 2010). When recording bubbles with shadowgraphy images, a characteristic bright spot in the centre of a bubble can be identified. The deformation of that spot allows to determine information of the bubble shape in the third dimension (Bongiovanni et al. 2000). Another approach is based on focused imaging with a small depth of field. Objects with increased distance from the focal plane are recorded blurry. This can be quantified and calibrated, which leads to an estimation on the distance from the focal plane (Pentland 1987). Recent works are applying this approach to microbubble flows (Cornel et al. 2018). In the presented study, this technique was adapted to the experimental setup and used to enhance the detection of bubble collisions.

Materials and Methods

A joining crossflow type T-junction with two inlets and one outlet is chosen as the object of investigation. The volume flow of both inlets is controlled by two pumps individually, as seen on the hydraulic scheme in Fig. 1a. Several sensors measure the operating parameters at the inlets and the outlet.

The T-junction model is illustrated in Fig. 1b. To guarantee optical accessibility, the model has plane and transparent walls with a rectangular cross section width $W = 25$ mm and depth $D = 5$ mm. At the downstream side connecting edge of the joining branch and the throughgoing straight branch, flow cannot follow the contour when deflected and detaches downstream of the corner. A recirculation area forms in the region of interest where bubbles are likely to interact. Because of the crossflow type narrow channel configuration, the flow pattern is complex and three dimensional. Therefore, bubble transport in all three directions is expected.

The bubbles are generated at a crossflow type T-junction microfluidic bubble generation unit which is supplied by syringe pumps. Bubbles with a diameter of $d_b \approx 500$ μ m get injected into the recirculation area via a needle through holes in the channel walls.

Downstream the model, the liquid is stored in a tank, which is equipped with a temperature control unit.

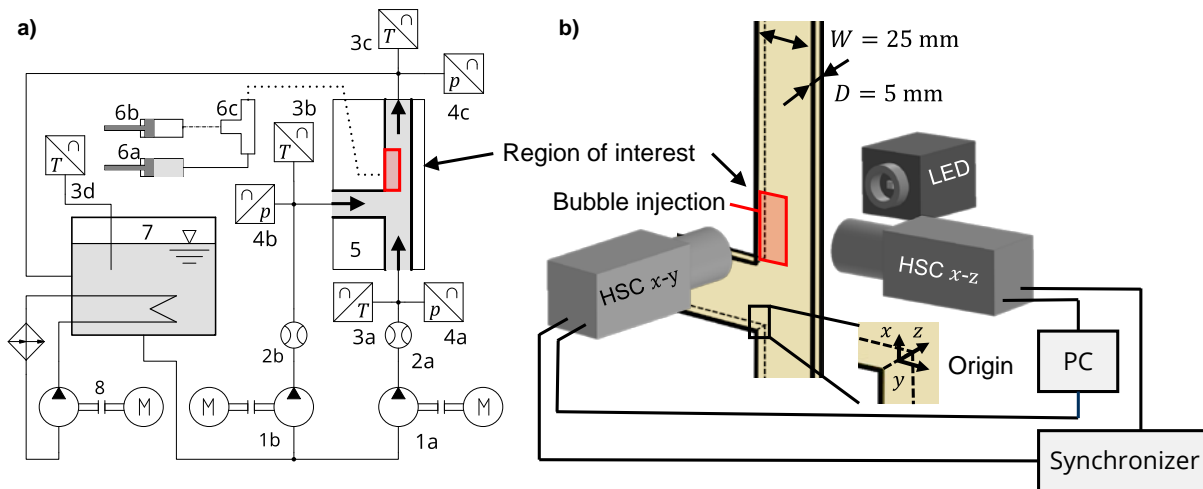


Fig. 1: Experimental setup: a) hydraulic scheme with pumps (1a, 1b), volume flow sensors (2a, 2b), temperature and pressure sensors (3a-d, 4a-c), T-junction (5), bubble generation unit (6a-c), tank with temperature control (7, 8); b) detailed view of T-junction with channel width W and depth D including location and orientation of the coordinate system and the setup of high-speed cameras (HSC) for the view at the x - y plane with backlight illumination from a LED and for the view at the x - z plane both controlled by a PC and triggered by a synchronizer; region of interest is marked in red in both images

The imaging was conducted from two perpendicular views using two high-speed cameras (Phantom Miro M 310, *Vision Research*, USA). The setup is shown in Fig. 1b. The front view camera with a lens (Nikkor 60 mm, *Nikon Corporation*, Japan) which yields a spatial resolution of $\Delta x = \Delta y = 20 \mu\text{m}/\text{px}$ records the x - y plane. The optical setup is characterized by a small depth of field where the focal plane is positioned in the middle of the channel ($z = 0 \text{ mm}$). Background illumination for this view is applied via a constant wave mode high performance LED (LED Head - LPS v3, *ILA_5150*, Germany). The side view camera with its lens (Nikkor 24-85 mm, *Nikon Corporation*, Japan) records the x - z plane with a spatial resolution of $\Delta x = \Delta z = 40 \mu\text{m}/\text{px}$. Due to the T-junction design, it was not possible to apply background illumination for the x - z plane. This leads to a decreased, but reasonable light intensity coming from the only light source as side illumination. Both cameras were synchronized and set to record with same temporal resolution which was chosen so that bubbles cannot move more than a fraction of their diameter ($100 \mu\text{m}$) between two frames.

The data evaluation was carried out with open-source software ImageJ and python image processing libraries *scikit-image*, *mahotas*, and *pytrack*. A scheme of the program chart is illustrated in Fig. 2. The greyscale images from the high-speed shadowgraphy method are sequentially arranged as single frames in an image stack and are processed by several steps. Firstly, a background image is created which represents the maximum intensity value for each pixel position in the whole stack. After the subtraction of the background image from each frame irregular background illumination and reflections from the wall are removed. A Gaussian filter suppresses small moving pollution without influencing the bubble edges due to the small radius of the filter. The key step of the pre-processing is the binarization of the images via a manually chosen threshold. The comparison of different threshold values with the original greyscale images must be considered to avoid both underestimation and overestimation of the bubble size. As the bubble images are characterized by a bright spot at their centres, a fill holes algorithm is included. Because not all pollution can be removed by the Gaussian filtering,

a size threshold is defined which removes objects with an area smaller than 100 px^2 corresponding to an equivalent diameter of $250 \mu\text{m}$. After an image inversion, the pre-processing outputs white bubbles on black background.

As the next step, the binarized images are processed in terms of the bubble parameters. The bubble position corresponds to the centre of mass of the object and the bubble equivalent diameter can be evaluated via the object size. It is necessary to consider more parameters in terms of a characterisation of the bubble shape and its change when interacting with other bubbles. This part of the routine is not discussed in detail in this work. Using the tracking routine, bubble velocity can be calculated. All parameters for each bubble in the corresponding frames are summarized in the bubble parameter list.

For the evaluation of bubble collisions, it is necessary to detect the movement of nearby bubbles towards each other before the collision takes place in order to describe the temporal sequence of the interaction. Therefore, all objects are dilated which means that the size is increased by a given value which is three pixels for the presented case. Then, the algorithm iterates every combination of bubble pairs and searches for an intersection, where two dilated objects are overlapping. If such an overlapping pair is found, certain conditions are checked to validate the event. Firstly, the two partners should both appear in the bubble parameter list for a reasonable number of frames to properly describe the temporal sequence of the process. Secondly, the bubbles should approach each other though the distance between the bubbles should decrease. Unfortunately, both criteria are valid for bubbles which are located in different depth positions where no contact is expected. With the presented routine, another validation criterion can be introduced by comparing the depth positions of the two partners.

When all criteria are checked, the event is registered and can be processed to describe the bubble temporal sequence of the interaction. In the following part, a routine is presented to estimate the depth coordinate from the greyscale images followed by the validation and the estimation of potential errors.

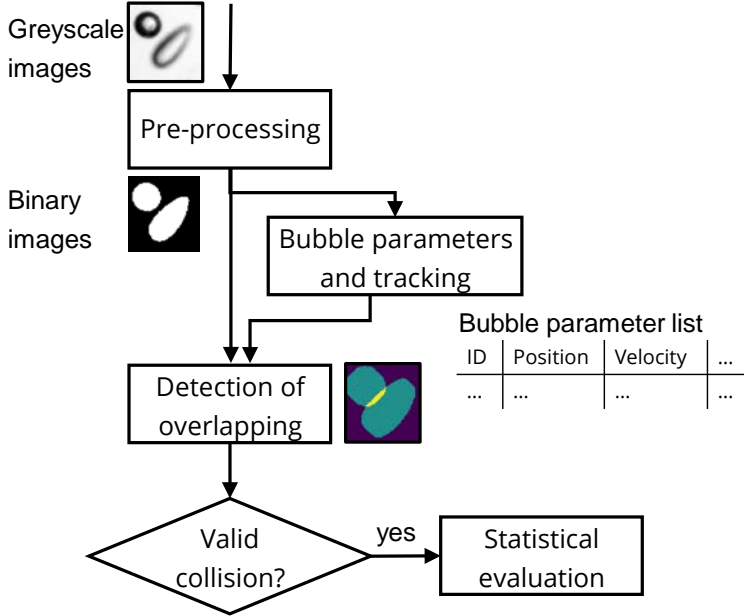


Fig. 2: Principal representation of the image processing program routine consisting of the pre-processing, the evaluation of bubble parameters, the bubble tracking, the detection of potential collisions, the validation criteria, and the summary for ongoing processing

The calibration curve gives the function of the edge strength depending on the distance between the edge and the focal plane, noted as l_z . For that purpose, shadowgraphy image

sequences of the x - y plane with the injection needle and rising bubbles in stagnated fluid at $z = 0$ mm were recorded. The bubbles are considered to rise in the centre of the channel. The distance was set by traversing the camera in z -direction. Fig. 3a shows the image at $l_z = 0$ mm. Varying the distance of the focal plane to the objects leads to a change in blur which is illustrated in Fig. 3b. The edge strength is evaluated using an image processing algorithm. To counteract the nonuniform illumination a background image is subtracted from the raw image at first. The bubbles must be segmented, and the images are normalized with the minimum and maximum pixel value of the whole image stack. The edge strength is obtained by the Sobel Operator which consists of a horizontal and a vertical filter which is convoluted with the images I :

$$G_h = \begin{bmatrix} -1 & 0 & +1 \\ -2 & 0 & +2 \\ -1 & 0 & +1 \end{bmatrix} * I, \quad G_v = \begin{bmatrix} -1 & -2 & -1 \\ 0 & 0 & 0 \\ +1 & +2 & +1 \end{bmatrix} * I.$$

Both filtered images are composed pixelwise via

$$G = \sqrt{G_h^2 + G_v^2}.$$

The maximum value of each image is extracted representing the edge strength $g = \max(G)$. Calculation of the mean value including the standard deviation for each image stack yields to the calibration function shown in Fig. 3c.

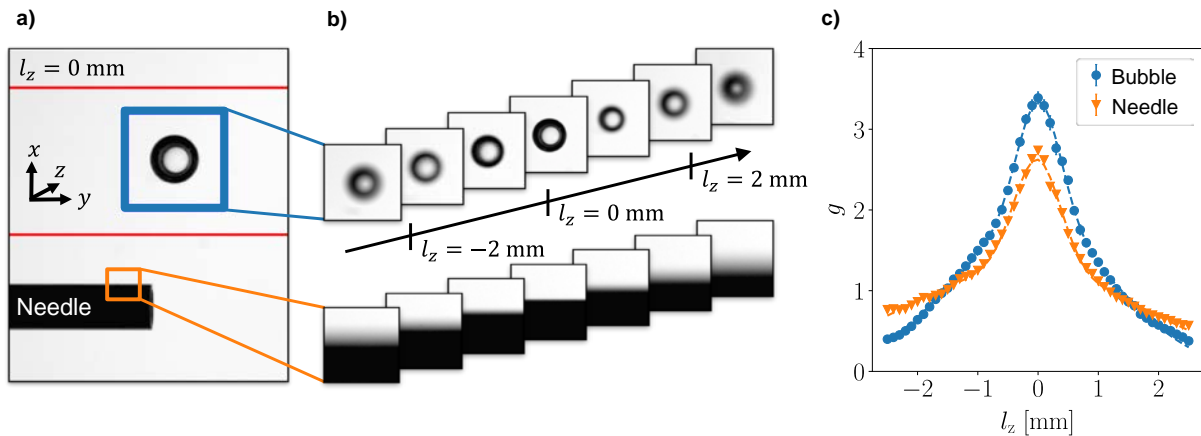


Fig. 3: Calibration curve of the optical system: a) shadowgraphy image of the x - y plane with the focal plane positioned at the middle of the channel at $l_z = 0$ mm showing the needle edge marked in orange and a rising bubble in stagnant fluid marked in blue as only bubble positions in between the red lines are considered; b) cropped images for different distances between the focal plane and the object l_z by traversing the camera position show the change in blur; c) evaluated normalized edge strength of the bubble and the needle for various positions in depth direction with superimposed Gaussian fit for illustration purpose

Error estimation of the determination of depth coordinate

A trajectory of one single bubble with coloured depth coordinate located in the recirculation area in the investigated flow configuration is shown in Fig. 4a. The evaluation of the z -coordinate takes place within the tracking algorithm. The calibration curve is input. Around the tracked bubble coordinates a background subtracted and normalized image is cropped. After applying the Sobel-Filter the maximum edge strength from this image is evaluated and the obtained parameter is matched with the calibration curve. Due to small differences in the normalization process, the evaluated edge strength can be slightly higher than the maximum value of the calibration function. For that case the evaluated z -position is set to $z = 0$ mm. To

estimate the z -coordinate, the values are interpolated from the points of the calibration curve and a negative and a positive value for one evaluated cropped bubble image can be found. Considering the calibration curve to be symmetric to the focal plane at $z = 0$ mm and neglecting the small skewness of the curve, the mean absolute value of the two z -coordinates is calculated. The differentiation between bubbles in the foreground or background by means of the bubble sharpness is not possible unless the considered bubbles are known to be located in front or behind the focal plane.

To validate the evaluated depth position from the calibration curve the side view (x - z plane) was recorded simultaneously together with the front view (x - y plane). The recording of the side view is evaluated with the same image processing routines. Because of the positioning of the LED resulting in illuminating the x - y plane, the bubble reflection spot in the centre could be segmented with more adequate accuracy than the outer bubble contour. This results in a small displacement of the depth coordinate in positive z -direction. The images depicting the x - z plane are binarized after applying a threshold and labelling. Fig. 4b shows an error estimation where the evaluated absolute z -coordinates from the front view (x - y plane) $|z_f|$ are plotted over the absolute z -coordinates from the side recordings (x - z plane) $|z_s|$. The coefficient of determination $R^2 = 0.986$ shows that this approach can lead to sufficiently accurate results.

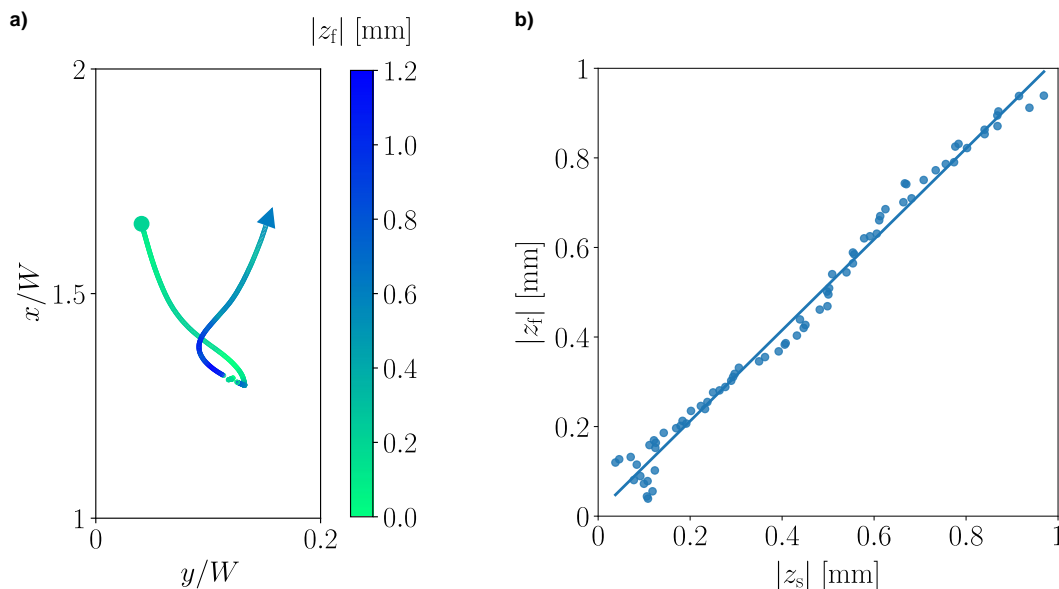


Fig. 4: 3D bubble trajectory: a) bubble locations in x - y plane coloured with absolute z -coordinate evaluated from imaging of the front view (x - y plane) $|z_f|$ using the presented routine; b) error estimation with evaluated, absolute z -coordinates from the front view (x - y plane) $|z_f|$ plotted over absolute z -coordinates from side recordings (x - z plane) $|z_s|$

The contribution of errors can be attributed to many of the following reasons. First, the accuracy of the coordinate movement determination is limited due to the magnification factor of the optical system. The different spatial resolutions of the two views result in errors in the estimation of the bubble position. Setting the threshold can lead to inaccurate determination of the centroid coordinates, too. Also, changes in the bubble contour can lead to centroid shift. The orthogonal positioning of the two high-speed cameras is also to be considered if the errors of the measurement method are discussed. Preceded assumptions were made to realize this method, like interpolating points between the calibration curve or neglect its asymmetry. By only considering the maximum edge strength of a cropped bubble image, skewed alignment of bubbles is neglected. When recording images to generate the calibration curve the assumption that bubbles rise in the channel centre might be another source of error. Another error is

due to reading off the traversing unit. The overall error of the presented method is estimated to be in the order of $\Delta|z_f| \approx 50 \mu\text{m}$.

Evaluation of bubble collisions

The presented routine will detect approaching bubbles by searching overlapping regions of objects with increased size. When evaluating the images, there are two situations which must be distinguished. Image sequences of those cases recorded from the view of the x - y plane are illustrated in Fig. 5. If two bubbles are located in different depth positions their projected trajectories can cross each other without any notable influence or interaction, as seen in Fig. 5a. Still, the bubbles will approach in the projected view so the routine will detect an overlapping region. Using the additional information on the z -coordinate for each bubble the distance between the two partners can be calculated with

$$l_b = \left| |z_{f,b1}| - |z_{f,b2}| \right| .$$

If the distance between the bubbles is smaller than 1.2 times the reference bubble diameter of $d_{b,r} = 500 \mu\text{m}$ it is presumed, that the bubbles will interact with another and a collision event is detected. This case is illustrated in Fig. 5b where two bubbles with high edge strength are colliding which leads to a deformation and a notable interaction. The results show, that with the presented routines, a differentiation between a collision and a falsely detected one is possible.

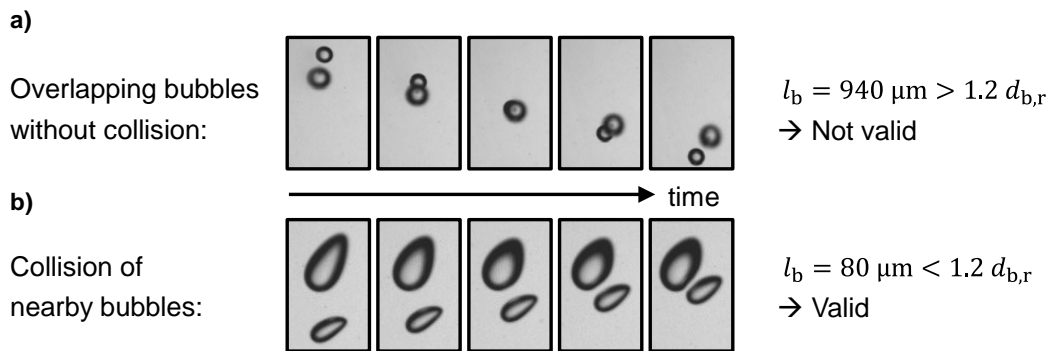


Fig 5: Examples of two cases to be distinguished: a) bubbles with overlapping projected trajectories without any notable interaction as expected from the different edge strengths indicating an increased distance in depth direction which is detected by the routine and labelled as not valid; b) collision of bubbles both characterized by sharp edges with a notable interaction in terms of bubble deformation which is detected by the routine as a valid collision

The distance between the bubbles l_b denotes the difference between the absolute values of the z -position. This leads to a systematic error if one bubble is located before the focal plane and one bubble behind. This issue can be overcome by constantly recording the perpendicular view to check the location of the bubble relative to the focal plane. The supporting recordings can be conducted with a much smaller temporal resolution. Therefore, an additional costly high-speed camera must not necessarily be used.

Conclusions

When studying bubble interaction, it is important to detect events like collisions, breakup, or coalescence. To achieve statistically relevant results a big number of interactions must be evaluated using automated image processing routines. For this purpose, an experimental facility was designed where bubbles get injected via injection spots and focused high-speed

shadowgraphy images can be recorded. The grayscale image sequences get processed with a presented routine which relies on basic image processing operations adapted for the present case. It is possible to evaluate parameters like position, size, and velocity for single bubbles. With the chosen optical setup, a small depth of field was achieved where bubbles are recorded with a notable blur with increasing distance from the focal plane. The relation between the edge strength of the bubble and the distance from the focal plane can be measured with a test configuration and was used as a calibration function to estimate the coordinate in z -direction when recording the x - y plane in the experiment. The estimated z -coordinate using the calibration function was validated using a second synchronized camera with a perpendicular view. A good agreement between the prediction of the absolute value of the z -coordinate from the front view (x - y plane) and the absolute value of the z -coordinate from the reference view (x - z plane) was attained. With the use of the pre-calibrated setup, it is possible to evaluate additional bubble parameters like the position and the velocity in the depth direction from the information of only one camera. Hence, it is possible to address highly three-dimensional multiphase flow problems in a cost-effective way. The evaluation of different regions of the bubble boundary together with the shape of the bright spot in the bubble centre would allow to state an approximation of the three-dimensional bubble shape.

Furthermore, a routine was presented to detect approaching bubbles and record the temporal sequence of the interaction. The estimation of the depth coordinate extends the validation criterion which filters possible collision events only if the bubbles are located in a defined distance in depth direction. The routine was tested with experimental data which showed that the expected differentiation was achieved. Implementing the presented routine for automated image processing allows to evaluate a big number of events and to get a statistically relevant data basis for future bubble interaction modelling.

Literature

Bongiovanni, C., Dominguez A., Chevaillier J.-P., 2000: Understanding images of bubbles. *Eur. J. Phys.* 21, 561

Cierpka C., Segura R., Hain R., Kähler C. J., 2010: A simple single camera 3C3D velocity measurement technique without errors due to depth of correlation and spatial averaging for microfluidics. *Meas. Sci. Technol.* 21, 045401

Cornel W., Westerweel J., Poelma, C., 2018: Local microbubble concentration by defocused volumetric shadowgraphy with a single camera. *Proceedings 18th International Symposium on Flow Visualization*

Pentland A. P. 1987: A new sense for depth of field. *Transactions on Pattern Analysis and Machine Intelligence*, Vol. PAMI-9, 4